ISSN: 0067-2904

Impact of Graphene Oxide Concentration and Anthocyanin Dye on the Structural, Morphological and Optical Properties of GO:TiO_2 Thin Films

M. J. AlSultani* , M. F. A. Alias
Physics Department, College of Science, University of Baghdad, Baghdad, Iraq

Received: 30/12/2023 Accepted: 10/7/2024 Published: 30/6/2025

Abstract

The aim of this research is to create thin films of GO:TiO_2 by the spray pyrolysis method. Hummer's method was utilized to prepare graphene oxide (GO). Different GO concentrations of (1, 2, 3, and 4) % were used, while a TiO_2 concentration was maintained at 4% to form films having various volume ratios of (1:4, 2:4, 3:4, and 4:4), which were then coated on FTO substrate at 400°C and later dipped into the pigment solution of anthocyanin (AD) obtained from red cabbage plant. Thin films' composition, structure, morphology and optical properties were studied through energy dispersive X-ray spectroscopy (EDX), X-ray diffraction (XRD), Fourier transform infrared (FTIR) microscopy, field emission scanning electron microscopy (FESEM) and UV-Vis spectrophotometry among other analytical techniques. The sizes of the crystals in these films were range from 15.6 nm to 19.38 nm and were characterized by polycrystalline structures with anatase phase. The FTIR spectra showed a functional group of all materials used in the range between 400 cm^{-1} and up to 4000 cm^{-1}. The surface morphology for GO:TiO_2 films showed randomly distributed aggregates or lumps of GO on the top surface of those films. As the GO concentration increased, a continuous network with TiO_2 was formed.

The optical properties and optical constants of the prepared GO:TiO_2 and GO:TiO_2:AD–thin films in the spectral range 300–1100 nm were examined. The absorbance increased, the direct energy gap decreased (its value is within 3.56–3.17 eV), and the optical conductivity increased with increasing the graphene oxide concentration. The energy gap values of GO:TiO_2:AD thin films, were less than that for GO:TiO_2. The results showed the presence of two energy gaps within the ultraviolet spectrum (3.31-3.12) eV and visible light ranges (2.32-2.14) eV. These results are good candidates for optoelectronic devices such as hybrid or dye-sensitized solar cells and photodetectors.

Keywords: GO:TiO_2 thin films, Anthocyanin dye, Structural properties, Morphological properties, Optical properties.

تأثير تركيز اوكسيد الكرافين و صبغة الانثوسيانين على الخصائص التركيبية والمورفولوجية والبصرية لأغشية GO:TiO_2 الرقيقة

محمد جاسم محمد السلطاني , ميسون فيصل أحمد الياس
قسم الفيزياء، كلية العلوم، جامعة بغداد، العراق

الخلاصة

*Email: sci.moh.j@environ.uoqasim.edu.iq

تركز هدف الدراسة على إنتاج أغشية رقيقة من $GO:TiO_2$ باستخدام تقنية الانحلال الحراري بالرش، حيث يتم تحضير أكسيد الجرافين (GO) بطريقة هامر. تم أخذ نسب مختلفة من GO (1، 2، 3، و4) %. مع تثبيت تركيز TiO_2 عند 4% لتكوين أغشية رقيقة بنسب حجمية (1:4، 2:4، 3:4، و4:4). تم ترسيب الأغشية على أرضية من أكسيد القصدير المشبع بالفلور (FTO). عند درجة حرارة 400 درجة مئوية، ثم يتم غمرها في محلول صبغة الأنثوسيانين المستخرج من نبات الملفوف الأحمر. يعد التحليل الطيفي للأشعة السينية المشتتة من الطاقة (EDX)، وحيود الأشعة السينية (XRD)، وتحويل فوريه للأشعة تحت الحمراء (FTIR)، و المجهر الإلكتروني الماسح للانبعاث المجالي (FESEM)، ومقاييس الطيف الضوئي للأشعة فوق البنفسجية والمرئية (UV–Vis) بعضًا من التقنيات التحليلية المستخدمة في الدراسة للنظر إلى تكوين الأغشية الرقيقة، وبنيتها، ومورفولوجيتها، وخصائصها البصرية على التوالي.

تمتلك الاغشية تراكيب متعددة البلورات بأحجام بلورية تتراوح من 15.6 إلى 19.38 نانومتر وبطور الانتاس . تظهرأطياف FTIR المجموعة الوظيفية لجميع المواد المستخدمة و لأغشية التي تحتوي على الأنثوسيانين بين 400 سم$^{-1}$ وحتى 4000 سم$^{-1}$. يُظهر التشكل السطحي لأفلام $GO: TiO_2$ مجاميع أو كتل من GO موزعة بشكل عشوائي على السطح العلوي لتلك الأفلام. مع زيادة تركيز GO، تكون هناك شبكة مستمرة بأشكال TiO_2.تحتوي اغشية $GO:TiO_2$ على شكل سطحي يحتوي على مجاميع أو قطع من GO متناثرة بشكل عشوائي على السطح العلوي. ومع زيادة نسبة GO، تتشكل شبكة مستمرة تحتوي على TiO_2.

تم فحص الخصائص البصرية والثوابت البصرية للأغشية $GO:TiO_2$ و $GO:TiO_2$:AD المحضرة قبل وبعد غمرها بالصبغة في المدى الطيفي 300–1100 نانومتر. بشكل عام، تزداد الامتصاصية مع زيادة نسبة أكسيد الجرافين. تقل فجوة الطاقة المباشرة بزيادة نسبة GO، وتكون قيمتها ضمن 3.56–3.17 الكترون. فولت، بينما تزداد الموصلية الضوئية. أن قيم فجوة الطاقة لأغشية $GO:TiO_2$:AD أقل من تلك للأغشية $GO:TiO_2$ فجوة الطاقة وقد أظهرت النتائج وجود فجوتين طاقيتين ضمن الطيف فوق البنفسجي (3.31–3.12) الكترون .فولت ومدى الضوء المرئي (2.32–2.14) الكترون. فولت. تعتبر هذه النتائج مرشحة جيدة للأجهزة الإلكتروبصرية مثل الخلايا الشمسية الهجينة أو الحساسة للصبغة وأجهزة الكشف الضوئي.

1. Introduction

The extraordinary properties and numerous uses of carbon nanostructures cover a vast area. Graphene, a carbon material with remarkable properties, has recently been the subject of much discussion [1, 2].

The exceptional thermal, electrical, and mechanical properties of graphene are due to its large specific surface area of 2620 m^2/g. At room temperature, the material demonstrates a much higher level of electrical conductance, as shown by an electron mobility value of 2.5 × 10^5 $cm^2/V.s$. Another feature is its thermal conductivity coefficient, close to 3000 watts per kelvin. Carbon atoms hybridised in the sp^2 form give graphene its unique planar structure. Flake graphite is primarily acknowledged as the predominant source of graphite in academic circles.

Graphene oxide (GO), a hydrophilic carbon material with non-conductive characteristics, is made by exfoliating graphite using strong oxidising chemicals [3, 4]. Despite its precise structural arrangement, graphene's previously infectious aromatic lattice is broken by epoxides, alcohols, ketones, and carboxylic groups in GO. The lattice is disrupted when the interlayer spacing increases, from 0.335 nm for graphite to more than 0.625 nm for GO [5,6]. Graphene oxide has received considerable attention due to its cost-effectiveness, convenient accessibility, and wide range of applications in the conversion of graphene [7].

Titanium dioxide (TiO_2) is considered a desirable wide-bandgap semiconductor, specifically classified as a transition metal oxide. It is non-toxic, exhibits exceptional stability, and demonstrates photoactivity by effectively absorbing light within the ultraviolet (UV) range [8].

Titanium dioxide shows notable resistance to corrosion and possesses favourable physical and chemical attributes, rendering it a promising material for solar cell applications [9,10]. Additionally, TiO_2 finds utility in gas sensors [11], biological sensors, and medical diagnostic applications [12].

Pure TiO_2 occurs in three distinct crystalline phases: anatase, brookite, and rutile. This group's anatase and rutile phases have a tetragonal shape, while the brookite phase has an orthorhombic form [13]. The anatase and rutile phases possess tetragonal symmetry, rendering them more appealing than the brookite phase [14]. Doping, quantum dots, and dyes are methods used to reduce TiO_2's energy gap and improve its ability to absorb light in the visible range [15]. The significance of point defects such as oxygen vacancies and titanium interstitials has also been investigated. Previous studies have indicated that introducing faults alters the electrical structure [16].

Anthocyanins, belonging to the flavonoid family, are a category of water-soluble pigments found in nature [17]. Carotenoids exhibit a wide distribution in the natural world, being present not only in the pigmented petals of flowers but also in many plant organs such as roots, stems, tubers, leaves, fruits, and seeds [18, 19]. This particular pigment exhibits a significant absorption level within the UV-visible range of the electromagnetic spectrum [20]. It is the primary factor influencing the manifestation of red-blue hues and their variations within the plant realm [21]. Anthocyanins exhibit inherent instability as a phenolic chemical, making extraction, storage, and processing operations intricate. Anthocyanins exhibit sensitivity to several conditions, such as temperature, light exposure, and pH levels [22]. Red cabbage is a notable source of anthocyanins due to its physiological activities and various applications [23].

This study uses the spray pyrolysis method to investigate the impact of GO concentration and anthocyanin natural dye (red cabbage) on the characterizations of TiO_2 thin films.

2. Experimental Part

2.1. Preparing GO

Graphene oxide was produced by the Hummer technique, as described in previous studies [24, 25]. Different amounts of 0.1, 0.2, 0.3, and 0.4 grams of graphene oxide were dissolved in 10 ml of acidified ethanol. To achieve acidification, 50 µl of concentrated hydrochloric acid was added to 10 ml of ethanol. The resulting solutions yield graphene oxide concentrations of 1%, 2%, 3%, and 4%, respectively.

2.2. Preparing TiO_2

6 ml of titanium tetraisopropoxide (TTIP), 1.2 ml of glacial acetic acid, 37 ml of deionized water, and 1 ml of concentrated nitric acid were mixed using a magnetic stirrer to create the precursor suspension; nitric acid was then slowly added to the solution. Following the initial mixing of the solution, TTIP was added drop-wise. The resulting mixture was then stirred for 30 minutes until it achieved clarity. Subsequently, the mixture was re-condensed at 80 °C for 90 minutes while maintaining constant stirring [26]. 0.4 grams of titanium (IV) nanopowder (supplied from Skyspring Nanomaterials, Inc., US), specifically in the anatase phase, was added to a suspension with 10 ml of precursor. Additionally, 250 µl of deionized water and 12 ml of acidic ethanol were added to the mixture. After 15 minutes of agitation, the solution underwent 480 seconds of sonication.

2.3. Preparing Anthocyanin Dye

Fifty grams of red cabbage leaves were chopped and put in a conical flask to which 100 ml of ethanol, 50 ml of acetone, and 50 ml of distilled water were added of (2:1:1) proportions. The conical flask was placed in a water bath at 50 °C for an hour. Three drops of hydrochloric

acid were then added to the dye extract and shaken well. Then, the solution was filtered using filter paper. The filtered solution was placed in a rotary evaporator at 100 °C and a rotation speed of 50 rpm to remove the ethanol, acetone, and distilled water solutions. After the time was up, the dye was still there. The solution was dried in an oven at 60 °C for 24 hours. Subsequently, 0.2 grams of the desiccated dye were dissolved in a solution of 40 ml of isopropyl alcohol, maintained at a temperature of 70 °C until complete dissolution was achieved. 3 ml of glacial acetic acid was added to the solution and stirred for 10 min, adding 50 µl of HNO_3 acid. The solution will turn red.

2.4. Preparing GO:TiO_2 Thin Films

The GO:TiO_2 suspensions were prepared using 1%, 2%, 3%, and 4% (w/v) of graphene oxide suspension concentrations with 4% (w/v) TiO_2 suspension. The volume ratios of GO:TiO_2 prepared in the experiment were 1:4, 2:4, 3:4, and 4:4. After stirring for 30 minutes, the mixtures underwent sonication for 5 minutes. Subsequently, the resulting mixture was sprayed onto a substrate made of fluorine-doped tin oxide (FTO) glass and heated to a temperature of 400 °, then immersed in the anthocyanin dye solution for 12 hours.

3. Results and Discussion

3.1. Compositions

The energy-dispersive X-ray analysis (EDX) spectrum of the GO:TiO_2-AD thin films with different GO concentrations (1, 2, 3, and 4) % deposited on FTO substrate using the spray pyrolysis technique are given in Figure 1. The analysis revealed the prominent presence of the components C, O, and Ti, along with the detection of other elements, including Sn and Si, which can be attributed to the FTO substrate, consisting of a SnO_2 layer and silica. Furthermore, a small percentage of impurities, such as phosphorus (P), sulfur (S), chlorine (Cl), and calcium (Ca), were identified as a result of the components utilized during the preparation process, as indicated in Table 1.

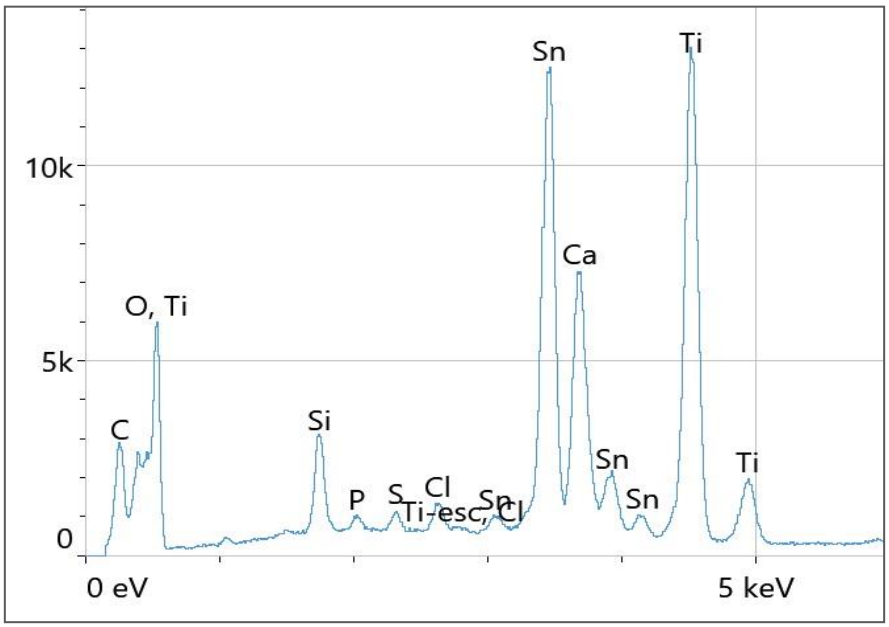

Figure 1: EDX spectrum of GO:TiO_2-AD thin film.

Table 1: EDX analysis for prepared films elements compositions.

Element	Weight %	Atomic %
C	10.3	23.0
O	31.8	53.4
Si	2.7	2.5
P	0.4	0.3
S	0.4	0.4
Cl	0.6	0.5
Ca	1.4	0.9
Ti	21.3	11.9
Sn	31.1	7.0

3.2. Structural Properties

3.2.1. X-Ray Diffraction

The X-ray diffraction (XRD) patterns of GO, TiO_2 powders, and GO:TiO_2 thin films deposited on FTO substrates were analysed, as shown in Figure 2. The produced GO exhibited a pronounced peak at 2θ = 11.7°, which refers to the (001) plane; additionally, a small peak can be noted at 2θ = 24.21° for the (002) plane, which is related to graphene [27].

The diffraction pattern of TiO_2 showed a maximum intensity peak at 2θ = 25.28° for the (101) plane, which corresponds to the anatase phase of TiO_2 [28] for tetragonal structure with a = b = 3.77 Å and c = 9.49 Å lattice constants according to the JCPDS card number # 00-002-0387.

The XRD of GO:TiO_2 thin films exhibited polycrystalline structure and distinct peaks at 2θ = 24.73°, 25.53°, 36.43°, 46.53° and 53.56° corresponding to the planes (002) (101), (004), (200) and (211), respectively. The optimum peak was observed at the (101) plane, corresponding to the anatase phase of the TiO_2. Also noted are peaks at 2θ = 32.51° and 50.39° of the (101) and (211) planes, respectively, corresponding to the FTO substrates [29].

The results depicted in Figure 2 indicate that no substantial alteration was observed of the diffraction pattern. The only change is that the single diffraction peak at about 11.7° in the GO spectrum disappeared; this makes a clear peak appear at 24.21°, caused by diffraction from the (002) crystallographic plane. This suggests that the water trapped within the material was eliminated during synthesis. Additionally, inter-sheet restacking, produced by Van der Waals forces, occurred. Furthermore, the ultrathin nanosheet establishes a conjugate network [30, 31]. Table 2 presents the computed values for several parameters, including interplanar spacing (d), lattice constants (a) and (c), crystallite size (D), dislocation density (δ), and microstrain (ε). The numerical values presented are derived from analysing the preferred (hkl) plane of the GO (001) and (101) for TiO_2 and GO:TiO_2 powders.

The interplanar spacing from Bragg's diffraction law was calculated using the below equation [32]:

$$d = \frac{n\lambda}{2\,sin\theta} \quad (1)$$

In the given context, the variable n is an integer, λ represents the wavelength of the incident X-ray, and θ is the Bragg angle. The preferred orientations of the GO:TiO_2 were found to be associated with the tetragonal structure. Consequently, the lattice constants (a) and (c) (where a = b ≠ c) for planes (200) and (004) were determined using the equation [32]:

$$\frac{1}{d^2} = \frac{h^2+k^2}{a^2} + \frac{l^2}{c^2} \quad (2)$$

The Scherrer formula was used to estimate the crystallite size [31]:

$$D = \frac{0.9\lambda}{\beta \cos\theta} \quad (3)$$

The parameter β represents the peak's Full Width at Half Maximum (FWHM). The length of dislocation lines per unit volume is defined as dislocation density, irregularity, and defects in the crystalline structure. The Williamson-Smallman method was employed to determine the dislocation density (δ) [33]:

$$\delta = \frac{1}{D^2} \quad (4)$$

where D is crystallite size.

Micro strain (ε) is measured to reveal details about the characteristics and structural composition of the material due to dislocations, grain boundaries, and other structural abnormalities in the crystal lattice [16]:

$$\varepsilon = \frac{\beta \cos\theta}{4} \quad (5)$$

The results indicated that D decreased with the increase of GO concentration, which means the surface area had increased, as higher surface area allows it to work efficiently as a photocatalyst. Also, when D decreased, ε and δ increased.

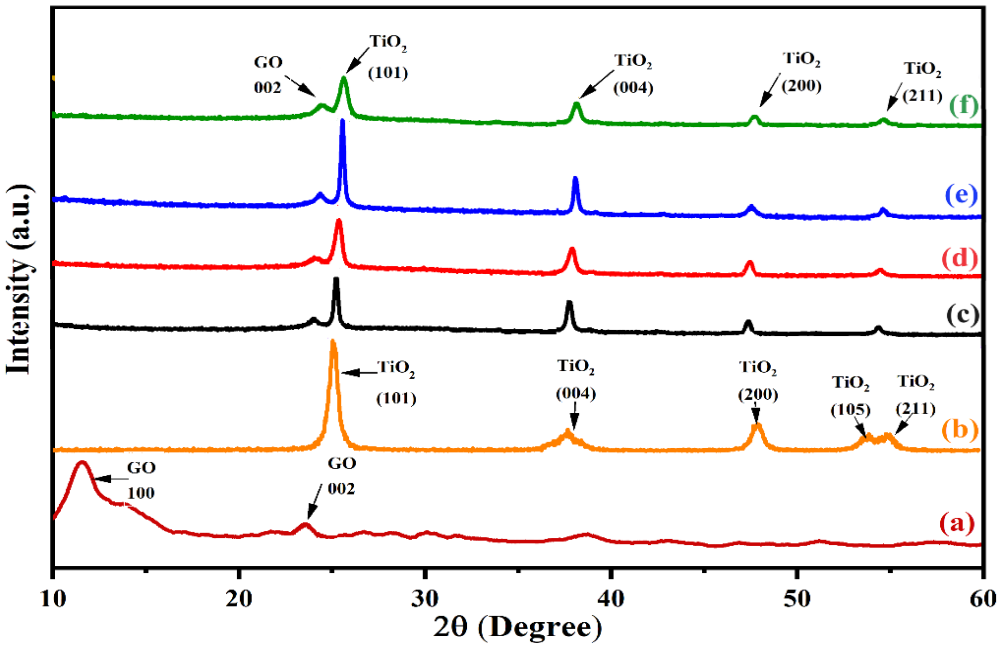

Figure 2: XRD patterns of (a) GO, (b)TiO_2 and (c-f) GO:TiO_2 thin films at different volume ratios (1:4 , 2:4 , 3:4 and 4:4), respectively.

Table 2: Structural parameters for prepared films with various GO concentrations.

Material	2θ (deg)	Structural parameters				Lattice constants	
		d_{101} (Å)	D (nm)	$\delta \times 10^{-3}$ $(nm)^{-2}$	$\varepsilon \times 10^{-3}$	a (Å)	c (Å)
TiO_2	25.28	3.51	15.65	4.08	2.21	3.78	9.49
1:4 GO:TiO_2	25.52	3.49	19.38	2.66	1.78	3.77	9.73
2:4 GO:TiO_2	25.51	3.49	18.52	2.91	1.87	3.77	9.67
3:4 GO:TiO_2	25.54	3.49	17.32	3.33	2.00	3.77	9.66
4:4 GO:TiO_2	25.53	3.49	16.61	3.62	2.09	3.77	9.66
Material	**2θ (deg)**	**d_{001} (Å)**	**D (nm)**	**$\delta \times 10^{-3}$ $(nm)^{-2}$**	**$\varepsilon \times 10^{-3}$**	**a (Å)**	
GO	11.7	7.57	4.64	46.4	7.46	7.5	

3.2.2. FTIR

The primary components of the organic portion of the dyes and GO consist of carbon, hydrogen, and oxygen. Figure 3 displays the FTIR spectra of TiO_2, GO, anthocyanin dye and GO:TiO_2-AD thin films in the 4000–400 cm^{-1} spectral range.

According to the vibrational analysis of TiO_2, Ti-O-Ti stretching vibration is noted at 480 cm^{-1}. The other vibration peak at 1621 cm^{-1} indicates the stretching vibration of Ti-OH [34].

GO spectrum exhibited many firm absorption peaks related to various oxygen functional groups. The peaks at 3430, 1730, 1636, 1389, and 1060 cm^{-1} are ascribed to the stretching vibration of the hydroxyl (OH) groups, carboxylate C=O stretching, the skeletal vibration of C=C, carboxyl C-O, and epoxide C-O-C or phenolic C-O-H, respectively. The presence of oxygen-containing functional groups, such as C=O and C-O, in the graphite confirms its oxidation into GO, which is compatible with the existing literature [35,36].

Anthocyanin dye spectrum showed strong absorption bands at 3430,1730,1636, 1449, 1340,1080 and 1020 cm^{-1}. The absorption bands indicate to OH, C=O, C=C, C-H, OH-CH_2, C-O-C and C-O functional groups, respectively, which are characteristics of anthocyanin [22].

All the GO:TiO_2-AD thin films with various GO concentrations exhibited a peak at 3430 cm^{-1}, which refers to the hydroxy-OH functional group. The band observed at 1740 cm^{-1} corresponds to the stretching of the C=O, and the band at 1678 cm^{-1} is attributed to the C=C bonds in the aromatic compounds. The presentation of C=C groups demonstrated the oxidation of graphite into GO and that the underlying layered structure of graphite is still retained. A band at 1485 cm^{-1} was also observed, associated with the deformation of the C-H bonds in the epoxy. Another band localized at 1430 cm^{-1} is due to OH-CH_2 bonds in the phenolic rings found in anthocyanin [34]. The band at 1336 cm^{-1} and 1026 cm^{-1} were correspond to the C-O and alkoxy C-O bonds, respectively. At the same time, the stretching vibration of the C-O-C esters is observed at 1149 cm^{-1}. The C-O-Ti bond at 810 cm^{-1} confirms the establishment of a connection between graphene sheets and TiO_2. The graphene oxide flake, which possesses a quinone structure, exhibits movement towards the surface of the semiconductor grain. Subsequently, the C-O-Ti bond was formed, leading to the transfer of electrons from the valence band to the carbon ring. The bond order of the C-O is enhanced during charge transfer. The emergence of an extra band C-O at 1336 cm^{-1} explains the occurrence of a new bond. Additionally, the bending mode of Ti-O-Ti and the deformative vibration of Ti-OH stretching mode can be observed at 483 cm^{-1} [27, 31].

Figure (4) illustrates schematic diagrams of the bonding between the surface of the TiO_2 grains with graphene oxide and anthocyanin dye. GO possesses different oxygen-containing functional groups, such as hydroxyl, epoxy, and carboxyl. These groups can interact electrostatically with TiO_2 to create a hybrid layer known as GO:TiO_2. The aromatic rings in anthocyanin dye molecules can engage in π-π^* stacking interactions with the graphitic domains seen in GO. On the other hand, anthocyanin dye molecules can be adsorbed onto the TiO_2 surface by interacting with the hydroxyl groups on anthocyanin and the TiO_2 surface, which frequently has hydroxyl groups or other reactive sites. GO functions as a highly conductive platform with a high surface area; TiO_2 functions as a photocatalyst or offers supplementary binding sites for the dye, whereas anthocyanin dye enhances the light absorption of TiO_2, making it very valuable in optoelectronics applications [37, 38].

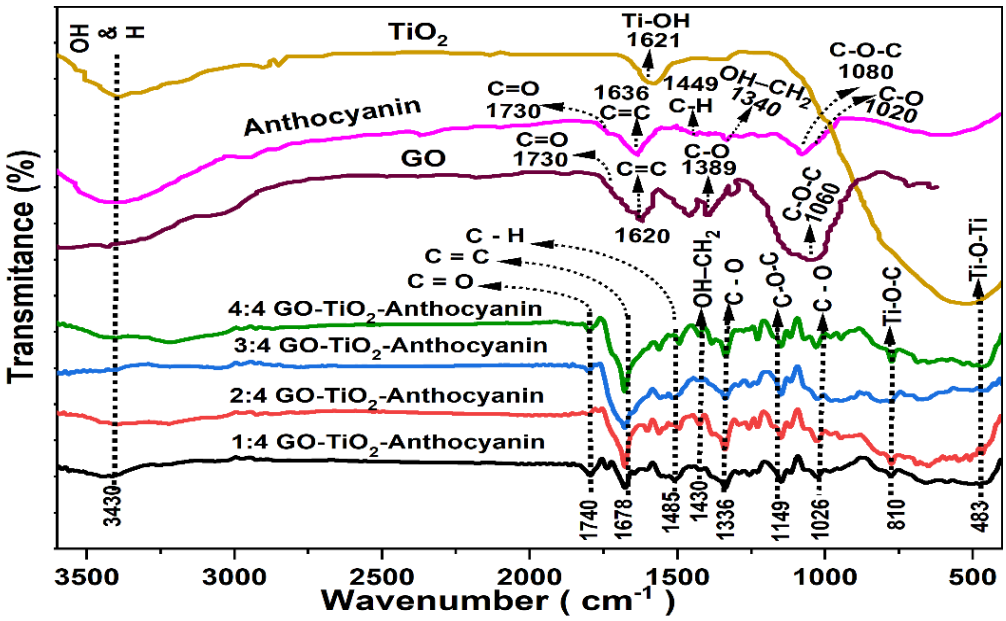

Figure 3: FTIR spectra of GO, TiO_2, anthocyanin dye and GO:TiO_2-AD thin films at different GO:TiO_2 volume ratios.

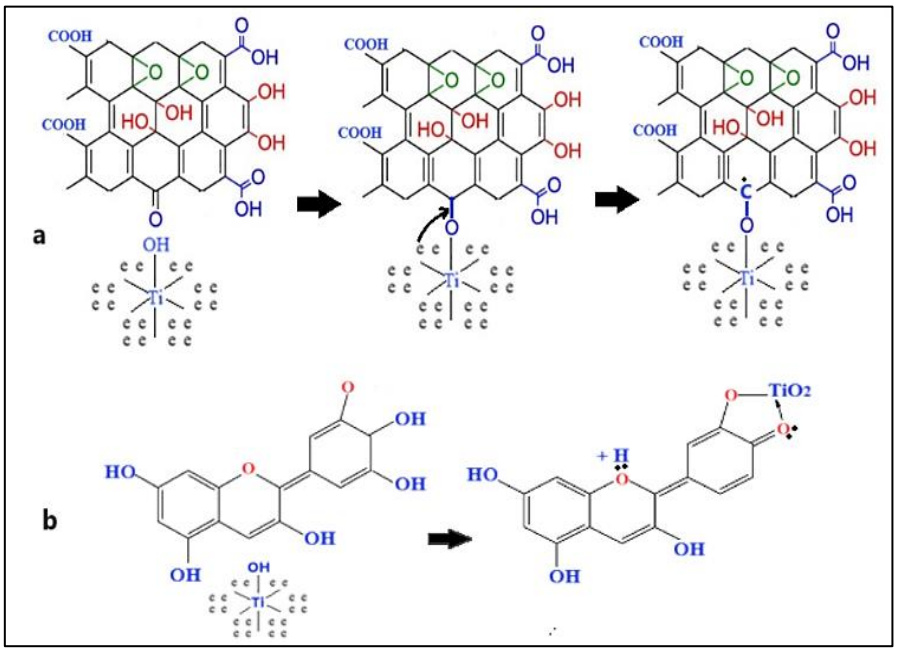

Figure 4: Schematic diagram of the mechanism of bonding between the surface of the TiO_2 molecules and (a) graphene oxide (b) anthocyanin dye.

3.2.3. *Morphological Properties*

Figure 5(a-e) shows FESEM images of TiO_2, GO:TiO_2-AD thin films at different GO:TiO_2 volume ratios (1:4, 2:4, 3:4 and 4:4).

It can be noted that GO:TiO_2 thin films have a common surface shape comprising many randomly placed chunks or aggregates of GO on the top surface of the films. The findings suggest that there was a tendency for GO to cluster and diffuse well in the GO:TiO_2 thin films. As the concentration of graphene oxide increased, it formed a continuous network with titanium dioxide. This network consists of pathways characterized by low electrical resistance, which permits the passage of charge carriers. The findings presented herein are consistent with the conclusions reached by Qiu et al. [27].

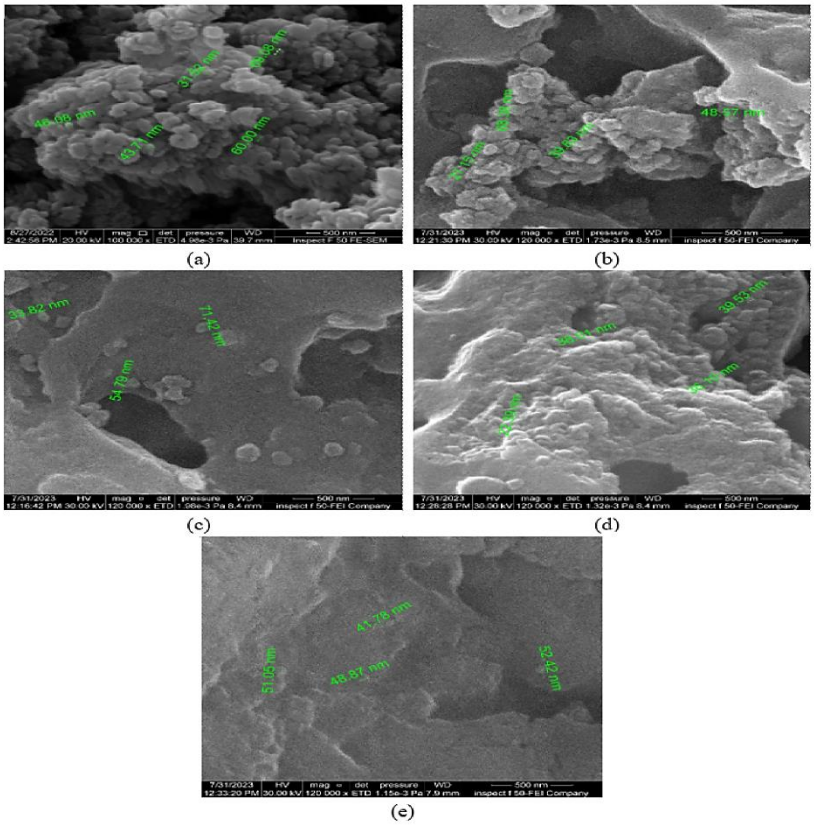

Figure 5: FESEM images of (a) TiO_2, (b-e) GO:TiO_2-AD thin films at GO:TiO_2 volume ratios of (1:4 , 2:4 , 3:4 and 4:4), respectively.

3.3. Optical Properties

The optical properties of thin films composed of GO:TiO_2 and GO:TiO_2-AD are analysed throughout the 300–1100 nm wavelength range, as illustrated in Figures 6 and 7. The results from Figure 6 indicated that for wavelengths less than 400 nm, the absorbance was high and then decreased with increasing wavelength. In contrast, the behaviour is the opposite for transmittance and reflectance. It can be noted that graphene oxide samples exhibited a higher capacity to absorb electromagnetic radiation at longer wavelengths than titanium dioxide. This implies that GO can potentially decrease the band gap of TiO_2. The findings showed that the unmodified TiO_2 possessed a band gap value of 3.58 eV [39, 13]. One can notice that the energy band gap of the GO:TiO_2 thin films decreased from 3.56 eV to 3.17 eV as the GO concentration was increased from 1% to 4%, respectively, as shown in Figure 7 and Table 4, where some unpaired electrons combine with the unbound electrons on the surface of TiO_2, resulting in the formation of a Ti-O-C structure. This decrease of the band gap is caused by the shifting up of the valence band edge. Additionally, the presence of graphene oxide facilitates the generation of Ti^{+3} and $O_{v,}$ which lowers the valence states generating intra-gap states; the energy levels of these states are lower than those within the band gap of TiO_2. Consequently, light absorption at higher wavelengths is enhanced [35].

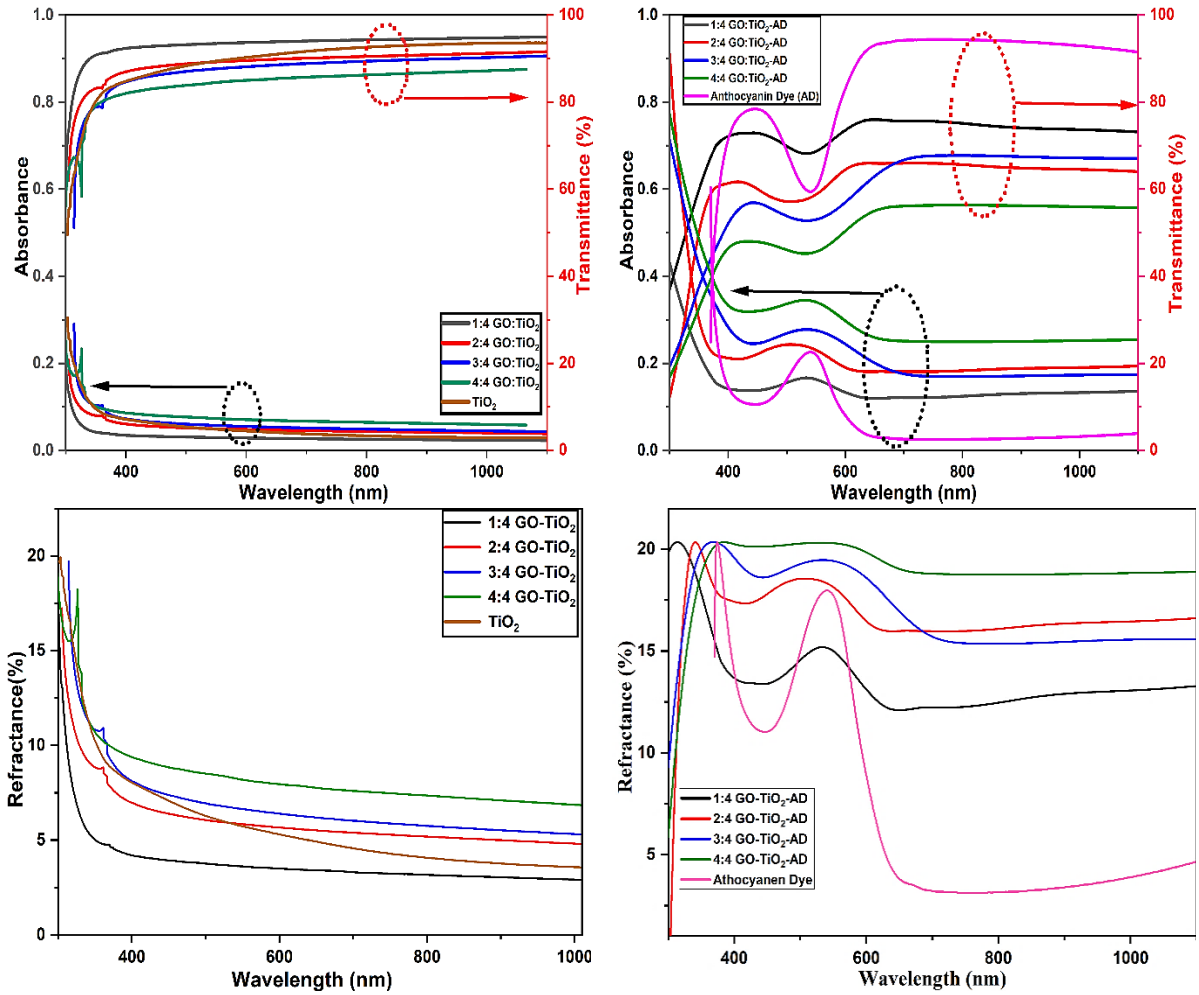

Figure 6: Variation of transmittance, absorbance and reflectance vs wavelength for GO:TiO_2 and GO:TiO_2-AD thin films

Figure 7 illustrates the variation of $(\alpha h\nu)^2$ with photon energy of GO:TiO_2 and GO:TiO_2-AD thin films. This figure indicates that all the prepared films have allowed direct energy gap. An improvement in the visible range of the electromagnetic spectrum when anthocyanin dye, a natural sensitizer, was added, can be observed; the energy gap of GO:TiO_2-AD thin films was in the range from 2.02 eV to 3.05 eV as the GO:TiO_2 volume ratio increased. These results agrees with that of other studies [40,41]. The chemical adsorption of these dyes onto the surface of TiO_2 is commonly acknowledged to result from the condensation of alcoholic-bound protons with the hydroxyl functional groups present on the nanocrystalline TiO_2 surface [37]. A significant shift of light absorption towards wavelengths exceeding 400 nm was seen. Anthocyanin dye contains chromophore groups within their chemical composition, enabling them to selectively absorb light within a particular area of the electromagnetic spectrum [17, 35]. The experimental findings demonstrated the presence of two separate energy gaps, one encompassing the ultraviolet wavelengths with values of 3.31 to 3.12 eV. The second energy gap is related to the visible wavelengths, with energy gap values from 2.32 to 2.14 eV. The process by which a group of anthocyanin forms a complex with graphene oxide is commonly known as chelation. This result has implications for the photocatalytic properties of GO:TiO_2 films when exposed to visible light [26]. The values of absorption coefficient (α), extinction coefficient (k), refractive index (n), real and imaginary dielectric constants (ε_r, ε_i), energy gaps (E_{g1}, E_{g2}), and optical conductivity(σ) [42] are listed in Table 4. Figure 8 illustrates band gap diagram for GO:TiO_2-AD thin films.

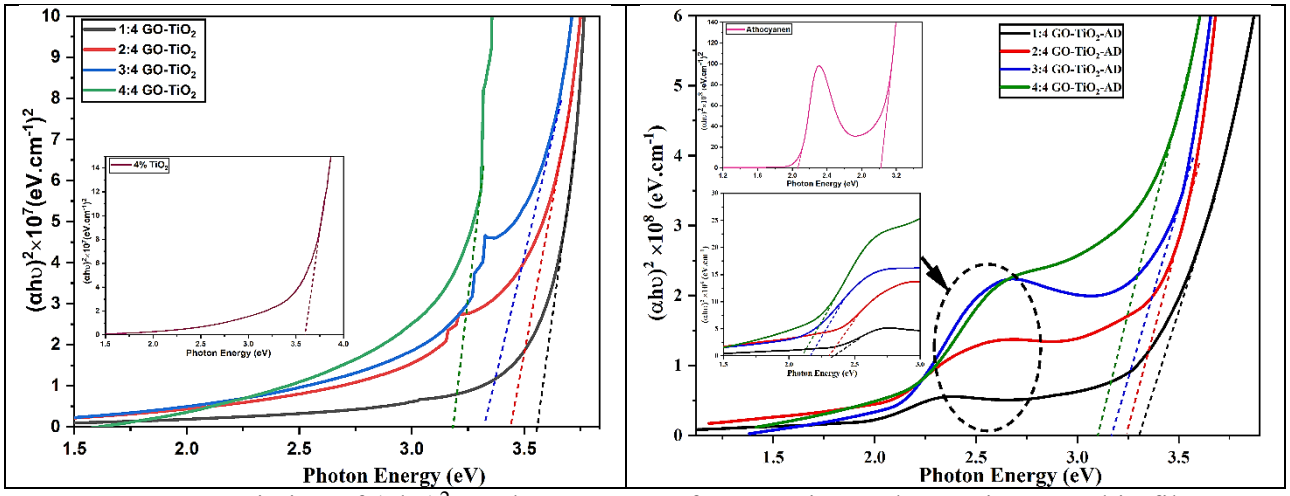

Figure 7: Variation of $(\alpha h\upsilon)^2$ vs photon energy for GO:TiO_2 and GO:TiO_2-AD thin films

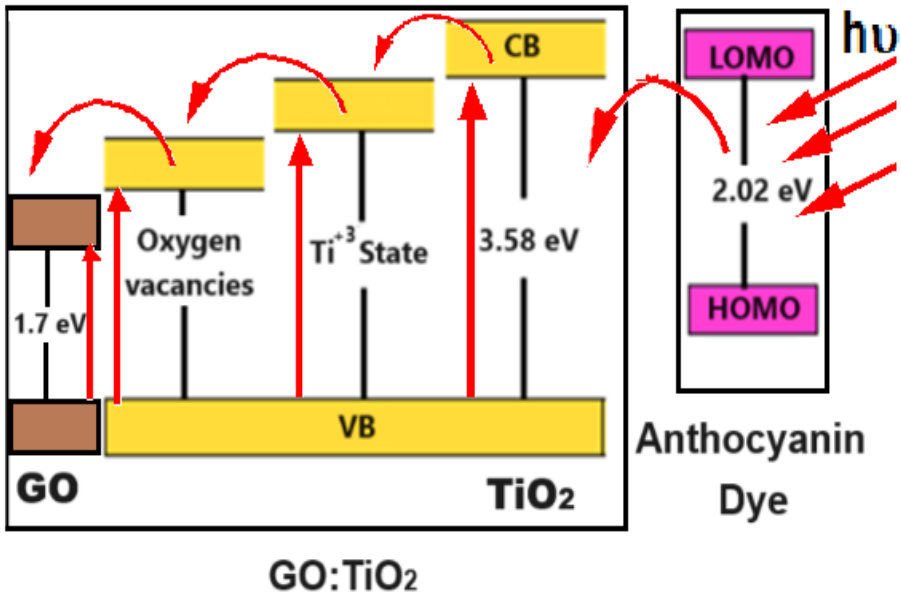

Figure 8: Band gap diagram for GO:TiO_2-AD thin films.

Table 3: Values of α, k,n, ε_r , ε_i ,Eg_1,Eg_2 and σ for GO:TiO_2 and GO:TiO_2-AD thin films

Sample	$\alpha \times 10^4$ (cm^{-1})	k	n	ε_r	ε_i	E_{g1} (eV)	E_{g2} (eV)	$\sigma \times 10^{13}$ (s^{-1})
TiO_2	0.190	0.0052	1.708	2.920	0.017		3.58	0.776
1:4 GO:TiO_2	0.077	0.0021	1.306	1.707	0.005		3.56	0.241
2:4 GO:TiO_2	0.145	0.0042	1.558	2.429	0.013		3.43	0.543
3:4 GO:TiO_2	0.159	0.0047	1.606	2.580	0.015		3.33	0.612
4:4 GO:TiO_2	0.186	0.0058	1.695	2.874	0.019		3.17	0.754
Anthocyanin Dye	0.247	0.0080	1.886	3.557	0.030	2.02	3.05	1.114
1:4 GO:TiO_2-AD	0.308	0.0092	2.053	4.216	0.037	2.32	3.31	1.512
2:4 GO:TiO_2-AD	0.4238	0.0128	2.303	5.305	0.059	2.28	3.25	2.331
3:4 GO:TiO_2-AD	0.525	0.0164	2.448	5.993	0.080	2.19	3.16	3.075
4:4 GO:TiO_2-AD	0.628	0.0198	2.521	6.359	0.100	2.14	3.12	3.786

4. Conclusions

GO:TiO_2 and GO:TiO_2-AD thin films successfully synthesized with different concentrations of GO were deposited on an FTO substrate using the spray pyrolysis deposition technique. The results showed the GO concentration effects on structural, morphological and optical properties of GO:TiO_2. XRD examinations confirmed the anatase phase with polycrystalline structure of GO:TiO_2 thin films. The crystallite size of prepared films increased with increasing the GO concentration. The GO:TiO_2 films showed a surface morphology of randomly dispersed aggregates of GO on the top surface. As the GO concentration increased, a continuous network with TiO_2 was formed. There was a tendency for GO to cluster and diffuse well in the GO:TiO_2 thin films. It is worth noting that increasing the GO concentration decreased the allowed direct energy gap values. As for the GO:TiO_2-AD thin films, the results showed two energy gaps within the ultraviolet and visible light ranges. These results are promising for the development of next generation optoelectronic devices, such as hybrid or dye-sensitized solar cells, and ultraviolet and visible detectors**.**

References

[1] A. K. Geim and K. S. Novoselov, "The rise of graphene," *Nature Materials*, vol. 6, no. 3, pp. 183–191, 2007.

[2] S. Saxena and T. A. Tyson, "Interacting quasi-two-dimensional sheets of interlinked carbon nanotubes: A high-pressure phase of carbon," *ACS Nano*, vol. 4, no. 6, pp. 3515–3521, 2010.

[3] A.Higginbotham, J. Lomeda, A. B. Morgan, and J. M. Tour, "Graphite oxide flame-retardant polymer nanocomposites," *ACS Applied Materials & Interfaces*, vol. 1, pp. 2256–2261, 2009.

[4] A. Lerf, H. He, M. Forster, and J. Klinowski, "Structure of graphite oxide revisited," *The Journal of Physical Chemistry B*, vol. 102, no. 23, pp. 4477–4482, 1998.

[5] H. He, J. Klinowski, M. Forster, and A. Lerf, "A new structural model for graphite oxide," *Chemical Physics Letters*, vol. 287, no. 1–2, pp. 53–56, 1998.

[6] C. Hontoria-Lucas, A. J. López-Peinado, J. de D. López-González, M. L. Rojas-Cervantes, and R. M. Martín-Aranda, "Study of oxygen-containing groups in a series of graphite oxides: physical and chemical characterization," *Carbon*, vol. 33, no. 11, pp. 1585–1592, 1995.

[7] A.Al-Shawi , M. Alias , P. Sayers and M. Fadhil Mabrook, "Improved memory properties of graphene oxide-based organic memory transistors", *Micromachines*, vol. 10, pp. 643, 2019.

[8] L.S. Chougala, M.S. Yatnatti, R.K. Linganagoudar, R.R. Kamble and J.S. Kadadevarmath," A simple approach on synthesis of TiO_2 nanoparticles and its application in dye sensitized solar cells," *Journal of Nano -and electronic Physics*, vol. 9, no. 4, p.6, 2017.

[9] I. O. Selyanin, A. S. Steparuk, R. A. Irgashev, A. V. Mekhaev, G. L. Rusinov, and A. S. Vorokh, "TiO_2 paste for DSSC photoanode: preparation and optimization of application method," *Chimica Techno Acta*, vol. 7, no. 4, pp. 140–149, 2020.

[10] A. K. Mohsin, S. D. Madhloom, and K. A. Aadim, "TiO_2/ZnO:Cu nanocomposite films in development the electrochemical potential for rechargeable batteries," *AIP Conference Proceedings*, 2022.

[11] S. Srivastava, S. Kumar, V. N. Singh, M. Singh, and Y. K. Vijay, "Synthesis and characterization of TiO_2 doped polyaniline composites for hydrogen gas sensing," *International Journal of Hydrogen Energy*, vol. 36, no. 10, pp. 6343–6355, 2011.

[12] S. M. Hunagund, Vani R. Desai, Delicia A. Barretto , Malatesh S. Pujar Jagadish, Kadadevarmath, Shyamkumar Vootla and Ashok H. Sidarai, "Photocatalysis effect of a novel green synthesis gadolinium doped titanium dioxide nanoparticles on their biological activities," *Journal of Photochemistry and Photobiology A: Chemistry*, vol. 346, pp. 159–167, 2017.

[13] H. Ennaceri M. Boujnah, A. Taleb, A. Khaldoun, R. S´aez-Araoz, A. Ennaoui, A. el Kenz, A. Benyoussef., "Thickness effect on the optical properties of TiO_2-anatase thin films prepared by ultrasonic spray pyrolysis: Experimental and ab initio study," *International Journal of Hydrogen Energy*, vol. 42, no. 30, pp. 19467–19480, 2017.

[14] M. Horn, C. F. Schwerdtfeger, and E. P. Meagher, "Refinement of the structure of anatase at several temperatures," *Zeitschrift für Kristallographie*, vol. 136, no. 3–4, pp. 273–281, 1972.

[15] C.E. Diaz-Uribe, A. Rodríguez, D. Utria, W. Vallejo, E. Puello, X. Zarate, E. Schott., "Photocatalytic degradation of methylene blue by the Anderson-type polyoxomolybdates/TiO_2 thin films," *Polyhedron*, vol. 149, pp. 163–170, 2018.

[16] S. A. Bhandarkar, Prathvi, A. Kompa, M. S. Murari, D. Kekuda, and R. K. Mohan, "Investigation of structural and optical properties of spin coated TiO_2:Mn thin films," *Optical Materials*, vol. 118, p. 111254, 2021.

[17] N. Ahmadiani, R. J. Robbins, T. M. Collins, and M. M. Giusti, "Anthocyanins contents, profiles, and color characteristics of red cabbage extracts from different cultivars and maturity stages," *Journal of Agricultural and Food Chemistry*, vol. 62, no. 30, pp. 7524–7531, 2014.

[18] H. Barani and H.Maleki,"Red cabbage anthocyanins content as a natural colorant for obtaining different color on wool fibers," *Pigment & Resin Technology*, vol. 49, pp. 229–238, 2020.

[19] S. Goulart, L. J. Jaramillo Nieves, A. G. Dal Bó, and A. M. Bernardin, "Sensitization of TiO_2 nanoparticles with natural dyes extracts for photocatalytic activity under visible light," *Dyes and Pigments*, vol. 182, p. 108654, 2020.

[20] A. Okello, B. O. Owuor, J. Namukobe, D. Okello, and J. Mwabora, "Influence of the pH of anthocyanins on the efficiency of dye sensitized solar cells," *Heliyon*, vol. 8, , p. e09921, 2022.

[21] B. Enaru, G. Drețcanu, T. D. Pop, A. Stănilă, and Z. Diaconeasa, "Anthocyanins: factors affecting their stability and degradation," *Antioxidants*, vol. 10, no. 12, p. 1967, 2021.

[22] H. da Silva, D. D. C. de Assis , A. L. Prada, J. O. C. S. Junior, M. B. de Sousa, A.M. Ferreira , J. R. R. Amado, H. D.O. Carvalho, A. V. T.de L.T. D.Santos and J. C. T. Carvalho., "Obtaining and characterization of anthocyanins from euterpe oleracea (açaí) dry extract for nutraceutical and food preparations," *Revista Brasileira de Farmacognosia*, vol. 29, pp. 677–685, 2019.

[23] N. Ghareaghajlou, S. Hallaj-Nezhadi, and Z. Ghasempour, "Red cabbage anthocyanins: stability, extraction, biological activities and applications in food systems," *Food Chemistry*, vol. 365, p. 130482, 2021.

[24] M. J. Alsultani, H. H. Abed, R. A. Ghazi, and M. A. Mohammed, "Electrical characterization of thin films $(TiO_2: ZnO)_{1-x}$ $(GO)_x$ / FTO heterojunction prepared by spray pyrolysis technique.," *Journal of Physics: Conference Series*, vol. 1591, no. 1, p. 012002, 2020.

[25] S. N. Alam, N. Sharma, and L. Kumar, "Synthesis of graphene oxide (GO) by modified Hummers method and its thermal reduction to obtain reduced graphene oxide (rGO)," *Graphene*, vol. 06, no. 01, pp. 1–18, 2017.

[26] A. C. M. San Esteban and E. P. Enriquez, "Graphene–anthocyanin mixture as photosensitizer for dye-sensitized solar cell," *Solar Energy*, vol. 98, pp. 392–399, Dec. 2013.

[27] J. Qiu, C. Lai, Y. Wang, S. Li, and S. Zhang, "Resilient mesoporous TiO_2/graphene nanocomposite for high rate performance lithium-ion batteries," *Chemical Engineering Journal*, vol. 256, pp. 247–254, 2014.

[28] S. Jamil and M. Fasehullah, "Effect of temperature on structure, morphology, and optical properties of TiO_2 nanoparticles," *Materials Innovations*, vol. 01, no. 01, pp. 22–28, 2021.

[29] M. K. Ahmad, N. A. Marzuki, C. F. Soon, N. Nafarizal, R. Sanudin, A. B. Suriani, A. Mohamed, M. Shimomura, K. Murakami, M. H. Mamat, and M. F. Malek, "Effect of anneal temperature on fluorine doped tin oxide (FTO) nanostructured fabricated using hydrothermal method," *AIP Conference Proceedings*, vol. 1788, p. 010001, 2017.

[30] Y.-C. Wang and C.-P. Cho, "Application of TiO_2-graphene nanocomposites to photoanode of dye-sensitized solar cell," *Journal of Photochemistry and Photobiology A: Chemistry*, vol. 332, pp. 1–9, 2017.

[31] P. Ribao, M. J. Rivero, and I. Ortiz, "TiO_2 structures doped with noble metals and/or graphene oxide to improve the photocatalytic degradation of dichloroacetic acid," *Environmental Science and Pollution Research*, vol. 24, no. 14, pp. 12628–12637, 2016.

[32] B. D. Cullity, *Elements of X Ray Diffraction*. Franklin Classics,2nd Ed. 2018.

[33] A. Timoumi, H. M. Albetran, H. R. Alamri, S. N. Alamri, and I. M. Low, "Impact of annealing temperature on structural, morphological and optical properties of GO:TiO_2 thin films prepared by spin coating technique," *Superlattices and Microstructures*, vol. 139, p. 106423, 2020.

[34] E. C. Prima, H. S. Nugroho, Nugraha, G. Refantero, C. Panatarani, and B. Yuliarto, "Performance of the dye-sensitized quasi-solid state solar cell with combined anthocyanin-ruthenium photosensitizer," *RSC Advances*, vol. 10, no. 60, pp. 36873–36886, 2020.

[35] L. I. Mohi and A. F. Abdulameer, "Optical investigation of reduced graphene oxide / Titanium dioxide nanocomposite thin films synthesized by hydrothermal method," *Iraqi Journal of Physics*, vol. 22, no. 1, pp. 75–81, 2024.

[36] T. M. Al-Saadi, M. A. Jihad," Preparation of Graphene Flakes and Studying Its Structural Properties", *Iraqi journal of science*, vol. 57, pp. 145-153, 2016.

[37] M. Kawa, A. Podborska, and K. Szaciłowski, "Interactions between graphene oxide and wide band gap semiconductors," *Journal of Physics: Conference Series*, vol. 745, p. 032102, 2016.

[38] R. Ramamoorthy, K. Karthika, A. Maggie Dayana, G. Maheswari , V. Eswaramoorthi, N. Pavithra, S. Anandan and R. Victor Williams, "Reduced graphene oxide embedded titanium dioxide nanocomposite as novel photoanode material in natural dye-sensitized solar cells," *Journal of Materials Science: Materials in Electronics*, vol. 28, no. 18, pp. 13678–13689, 2017.

[39] A. T. Raghavender, A. P. Samantilleke, P. Sa, B. G. Almeida, M. I. Vasilevskiy, and N. H. Hong, "Simple way to make Anatase TiO_2 films on FTO glass for promising solar cells," *Materials Letters*, vol. 69, pp. 59–62, 2012.

[40] P. Amin, F. Muhammadsharif, S. Saeed, and K. Sulaiman,"A study on the optoelectronic parameters of natural dyes extracted from beetroot, cabbage,walnut, and henna for potential applications in organic electronics," *Journal of Fluorescence*, vol. 32, pp. 203–213, 2021.

[41] A. R. Woldu, D. W. Ayele, N. G. Habtu, and Y. A. Tsigie, "Anthocyanin components for dye-sensitized solar cells extracted from Teclea Shimperi fruit as light-harvesting materials," *Materials Science for Energy Technologies*, vol. 3, pp. 889–895, 2020.

[42] Z. N. Kayani, M. Saleem, S. Riaz, S. Naseem, and F. Saleemi, "Structure and optical properties of TiO_2 thin films prepared by a Sol-Gel processing," *Zeitschrift Für Naturforschung. A, a Journal of Physical Sciences*, vol. 74, no. 7, pp. 635–642, 2019.